Ultra-Compact 50 W Flat Supercontinuum Generation in Single-Stage Self-Q-Switched Fiber Laser With Photonic Crystal Fiber

Jiuru He, Rui Song, Li Jiang, and Jing Hou

***Abstract*—An all-fiber supercontinuum (SC) laser source with 50.7 W average output power and spectrum ranging from 500 nm to 2400 nm is demonstrated. With the generation of high peak power nanosecond pulses and photonic crystal fiber (PCF) in the self-Q-switched fiber laser, the output SC shows good spectral width and flatness which has a 20 dB bandwidth of 1900 nm except the 1064 nm peak. The effect of the PCF length on the spectral characteristics and output power of SC were carefully studied. To the best of our knowledge, this is the highest power of SC generated in a single-stage fiber laser with such a broadband spectrum. This ultra-compact SC generation method has the merits of simple structure, low cost and good robustness, which provide an easily available SC generation method for various practical applications.**

***Index Terms*—Supercontinuum, photonic crystal fiber, self-Q-switched, fiber laser.**

I. Introduction

SUPERCONTINUUM (SC) generation is a complex process involving various nonlinear effects, such as self-phase modulation (SPM), cross phase modulation (XPM), modulation instability (MI), stimulated Raman scattering (SRS) and so on, which can strongly broaden a narrowband input spectrum to dozens or even thousands of nanometers. Since the first experimental observation in 1970 [1], SC has been studied extensively and achieves broad applications in the fields of biophotonics, hyperspectral lidar, optical communications and biomedical imaging [2]–[5]. Besides, the brightness of SC has been confirmed to be orders of magnitude higher than the thermal radiation sources and the square mile large synchrotrons which can have a great impact on applications within spectroscopy and microscopy [6].

Manuscript received January 18, 2022; revised February 22, 2022; accepted February 28, 2022. Date of publication March 3, 2022; date of current version March 31, 2022. This work was supported by the State Key Laboratory of Pulsed Power Laser Technology under Grant SKL2019ZR02. (*Corresponding authors: Rui Song; Jing Hou.*)

Jiuru He, Li Jiang, and Jing Hou are with the College of Advanced Interdisciplinary Studies, National University of Defense Technology, Changsha 410073, China, and also with the State Key Laboratory of Pulsed Power Laser Technology, Hefei 230037, China (e-mail: 13526287676@163.com; 17815936261@163.com; houjing25@sina.com).

Rui Song is with the College of Advanced Interdisciplinary Studies, National University of Defense Technology, Changsha 410073, China, with the State Key Laboratory of Pulsed Power Laser Technology, Hefei 230037, China, and also with the Key Laboratory of Atmospheric Optics, Anhui Institute of Optics and Fine Mechanics, Chinese Academy of Sciences, Hefei 230031, China (e-mail: srnotice@163.com).

Digital Object Identifier 10.1109/JPHOT.2022.3156105

The creative invention of photonic crystal fiber (PCF) with controllable dispersion profiles and high nonlinearity is a significant milestone for the development of SC [7]. Currently, using a pulsed laser from femtosecond to nanosecond regime to pump a piece of PCF is commonly used for broadband SC generation [8]–[10]. Q-switching and mode-locking techniques are well-developed and widely used to obtain high peak power laser pulses [11]–[16]. For the Q-switching scheme, the experimental configuration is usually complicate and expensive (e.g., acoustic optical modulator (AOM) and additional integrated electronic circuits are always incorporated in the actively Q-switched fiber laser) [12], [13]. For the mode-locking technique, methods like semiconductor saturable absorber mirror (SESAM) and nonlinear polarization rotation (NPR) are widely used [14]–[16]. Undoubtedly, the using of the above technologies in SC generation would complicate the structure, which also inevitably increase the system cost and easily affected by the environment. Besides, the average output power directly from a pulsed laser remained relatively low. Thus, to obtain high power SC output, a multi-stage amplification is necessary to amplify the average power of the pulsed laser seed to a high level. In Ref. [8], by pumping the PCF with a picosecond fiber in three-stage master oscillator power amplifier (MOPA) configuration, a SC with 39 W output with spectral range covering from 600 nm to beyond 1700 nm was demonstrated. In 2018, Qi *et al.* also using a multi-stage MOPA configuration to amplify a 1016 nm pulsed seed, an 80 W SC with spectrum from 350 nm to 2400 nm was realized [9]. The multi-stage MOPA configuration can effectively amplify the average power of the pulsed laser seed to obtain a high power SC output, but it also increases the complexity and difficulty of the system.

Another common used method for SC generation is using a continuous-wave (CW) laser to pump a piece of PCF [17]–[23]. Comparing with the pulsed pumping scheme, it has the distinct advantages of simple structure and higher average output power. However, it also has the defect of lower peak power, which causes the less broadening of SC and the requirement for longer fiber length to enhance the nonlinear interaction. Specially, the spectral broadening toward the short wavelength side is quite difficult [17]–[20]. To solve this issue, gain-switched CW fiber laser could be a strongly competing technology, which not only can obtain a broader SC output but also has the merit of simple structure [22], [23].

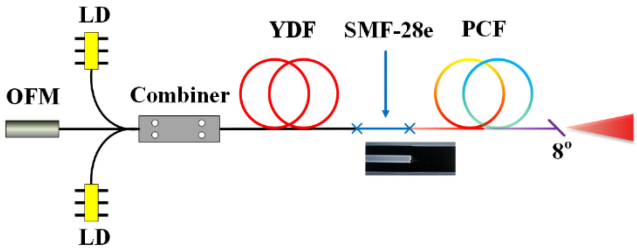

Fig. 1. Schematic diagram of the proposed SC laser. LD, laser diode; OFM, optical fiber mirror; YDF, ytterbium-doped fiber; PCF, photonic crystal fiber.

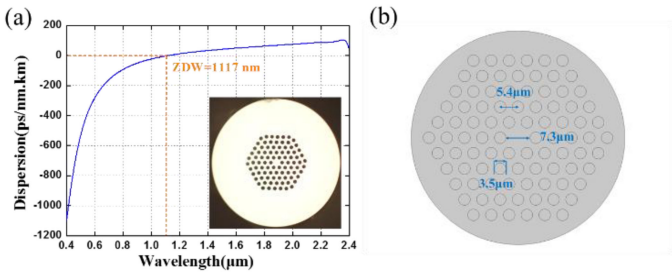

Fig. 2. (a) Calculated dispersion curve of the PCF. Inset: microscope image cross section of the PCF. (b) the measurement data of the PCF.

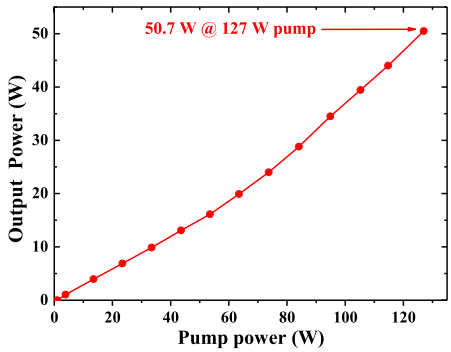

Fig. 3. Output power versus pump power.

In this manuscript, we report a high power 50.7 W SC generated in a self-Q-switched fiber laser. By the combined effects of the nanosecond pulses and the PCF, a flat SC spanning from 500 nm to 2400 nm with 20 dB bandwidth of 1900 nm is demonstrated. Further experimental researches are carried out to investigate the effect of the fiber length on SC generation. To the best of our knowledge, it is the highest power of SC generated in a single-stage fiber laser with such a broadband spectrum.

II. Experimental Setup

Fig. 1 shows the experimental setup. The proposed ultra-compact SC laser mainly includes two parts: the first part is based on a passively Q-switched ytterbium fiber laser which we have a detailed analysis in Ref. [24]; the second part is the nonlinear medium for spectral broadening which we used here is a piece of PCF. For the self-Q-switched ytterbium fiber laser, it adopts a half-opened cavity configuration. Two 976 nm multimode laser diodes (LDs) are used here and they have a combined 127 W pump power. The two LDs are spliced respectively to the arms of a $(2+1) \times 1$ pump and signal combiner to pump the double clad ytterbium-doped fiber (YDF). In order to obtain high power output, the length of the YDF is optimized to 4.5 m. The core/cladding diameter of the YDF is 10/125μm respectively, and its absorption coefficient at 976 nm is about 4.23 dB/m. An optical fiber mirror (OFM) which has a 40 nm reflection bandwidth and a central wavelength of 1064 nm is spliced to the signal port of the combiner to provide broadband feedback. The above mentioned fiber and devices constitute this compact self-Q-switched ytterbium fiber laser and the detailed analysis of its output characteristics in frequency and time domain are presented in Ref. [24].

Then the output of the self-Q-switched pulsed laser is launched into a section of 9-m-long PCF. The inset of Fig. 2(a) gives the micrograph cross section of the PCF. The PCF has a core diameter of 7.3 μm. And its air-hole pitch and air-hole diameter are also measured to be 5.4 μm and 3.5 μm respectively, as shown in Fig. 2(b). The graph shown in Fig. 2(a) depicts the dispersion curve of the PCF which is calculated by the fully vectorial finite-element method. It can be seen that the zero-dispersion wavelength (ZDW) is located at 1117 nm. In order to reduce the splicing loss caused by the severe mode field mismatch between the YDF and the PCF, a 0.3-m-long 8.2 μm/125 μm (core/cladding diameter) SMF-28e is utilized here as the transition fiber. The splicing point between the SMF-28e and PCF should be handled properly to ensure the stability and reliability of the system with high-power operation. For this purpose, the parameters of the fusion splicer such as the discharging position and the discharging intensity are optimized to achieve a robust splicing joint. A several milliwatts continuous laser at 1064 nm was used to estimate the splicing loss which shows that the transmission rate of this point is ~94%. The splicing joints, the YDF and the PCF were all placed on a metal cooling plate for heat dissipation. At the output port, the end of the PCF is angle cleaved to prevent unexpected feedback.

III. Experimental Results and Discussions

A. Performance of the High Power SC Source

The output power of this ultra-compact SC laser was detected by a power meter (Ophir, L50A-LP2-35). The output power almost increases linearly with the increase of the pump power at the start, as shown in Fig. 3. When the pump power reaches 63.5 W, the output power increases a little faster. More energy accumulation at the spectral peak near 1064 nm is the reason for this phenomenon, which can be verified latter in Fig. 4. When the incident pump power is 127 W, a maximum output power of 50.7 W was obtained, corresponding to an optical-to-optical conversion efficiency of up to 40%.

The output spectrum was recorded by two different optical spectrum analyzers (YOKOGAWA, AQ6374 for 400-1600 nm and AQ6375 for 1600-2400 nm), respectively. In order to prevent the multi-order interference when measuring the 1600-2400 nm band, a long-pass filter with a cutoff wavelength of 1200 nm was used. Fig. 4 illustrates the spectral evolution of SC with

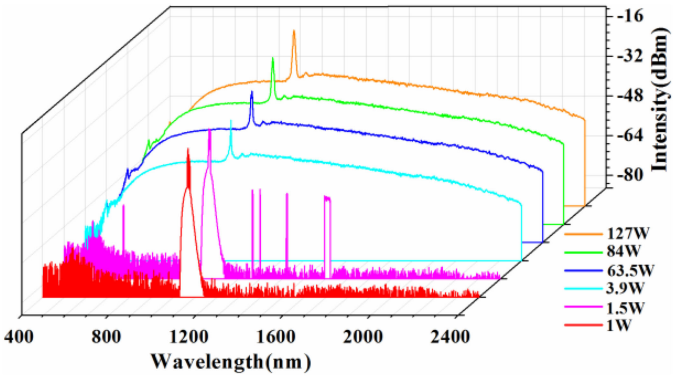

Fig. 4. Recorded spectra with different pump powers.

different pump power. When the pump power is 1 W, amplified spontaneous emission (ASE) with parasitic laser spikes is demonstrated in the red curve [25]. With the pump power further increasing, a few spectral spikes with narrow bandwidth and different locations are superimposed randomly on the output spectra (magenta curve in Fig. 4). In such cases, the spectral spikes appear randomly in the whole spectral band with every spectral measuring, and it will occur more frequently with a little increasing of the pump power. The variation of the spectral spikes could be induced by the self-induced laser line sweeping (SLLS) effect which is featured by narrow laser line and self-scanning of the laser wavelength spanning the whole spectral band [26], [27]. The generation of the Stimulated Brillouin Scattering (SBS) stokes can also benefit from the narrow line width of the SLLS effect [28]. When the pump power reaches 3.9 W, a wide and flat SC is generated. Nevertheless, with the pump power further increasing, the SC didn't show obvious spectral broadening. This may be attributed by the attenuation of PCF in both the long and short wavelength directions, or the limited peak power of the pump pulses. Meanwhile, the spectral peak in the output spectra near 1064 nm get slightly wider and higher with the pump power increasing. Dual or multi wavelengths pumping may be a good solution to solve this issue which can effectively improve the spectral flatness of SC [29], [30]. Especially, due to a big portion of the power remains at the 1064 nm peak, so the power spectral density (outside the 1064 nm peak) might be relatively low. Fig. 5(a) shows the power spectral density of SC at the maximum pump power versus wavelength. Numerical integration of the SC spectrum indicates that the power proportion of the 3 dB bandwidth of 1064 nm peak accounts for 30.2% of the total SC power. For comparison, the spectral power density of SC in our previous work [24] is also given in Fig. 5(b).

Fig. 6 gives comparison of the spectrum between the pump power of 3.9 W and the maximum pump power of 127 W. Under the 127 W pump power, a high power 50.7 W SC ranging from 500 nm to beyond 2400 nm is obtained and it has an excellent spectral flatness which has a 20 dB bandwidth of 1900 nm except the 1064 nm peak. With the feedback from the OFM, the main peak wavelength ω (1064nm) is identical with its central wavelength. In the process of SC generation, various

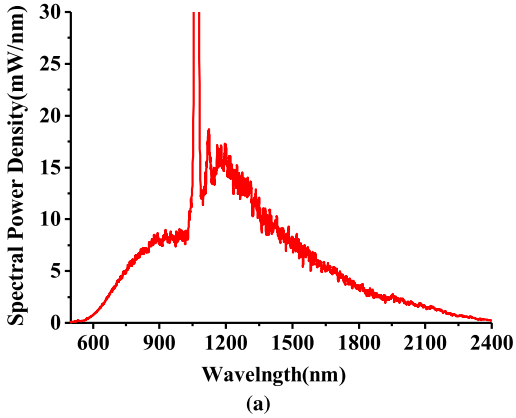

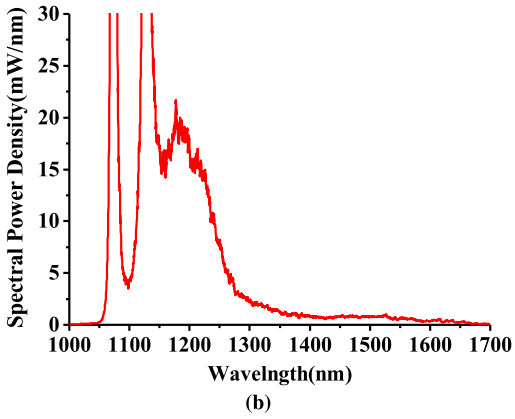

Fig. 5. The spectral power density of SC at the maximum pump power versus the wavelength: (a) the experimental results in this paper, (b) Our previous work in Ref. [24].

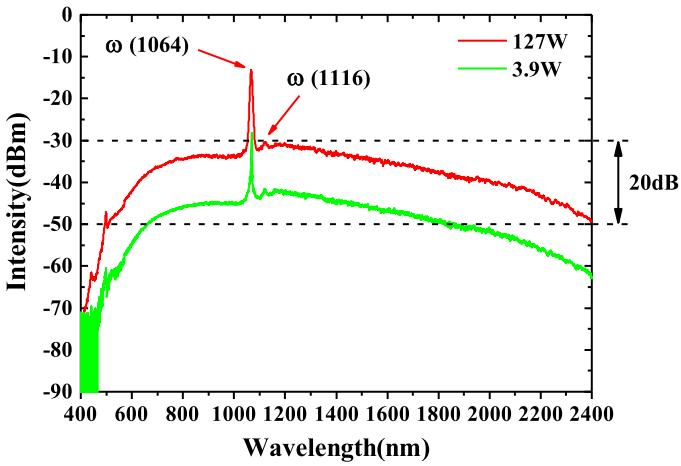

Fig. 6. Comparison of the spectrum between the pump power of 3.9 W and 127 W.

nonlinear effects work in coordination and lead to the broadening of the spectrum. Another tiny peak wave ω (1116 nm) can also be noticed in the output spectrum. This can be attributed to the stimulated Raman scattering (SRS) effect as the 1064 nm pump peak is located in the normal dispersion region of the PCF. After the spectrum reaching and rising above the ZDW of the PCF by SRS effect, Modulation instability (MI) gives birth

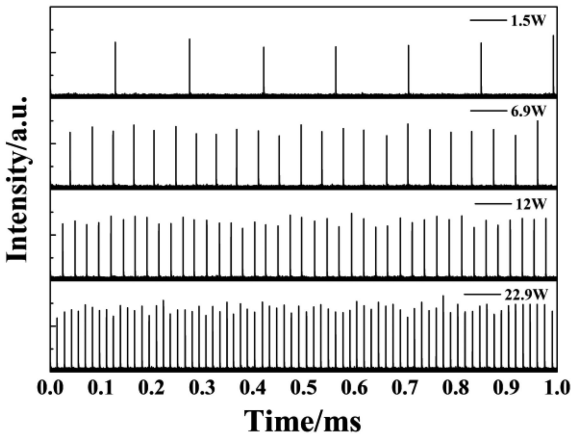

Fig. 7. The time domain output under different pump power.

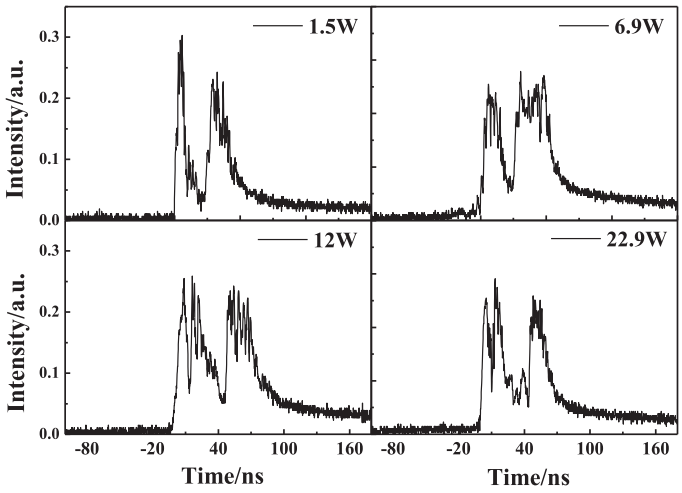

Fig. 8. Pulse shapes under different pump power.

to a great deal of solitons. Then the solitons undergo soliton self-frequency shift (SSFS) mechanism which can effectively induce the continuum broadening to more than 2400 nm. At the same time, four wave mixing (FWM) effect and dispersive wave generation comes into play to extend the spectrum to the short wavelength region. In the spectral profile, some small protrusions can be also noticed in the short wavelength side. This demonstrate that the phase matching condition and group velocity matching condition of the FWM can be satisfied in this process. As this pump/fiber setup is similar with that used in Ref. [23], [32], the spectral bandwidth of the generated SC will not change if slight variation in the pump wavelength or the ZDW occur. This is because as the pump is effectively transferred into the long wavelength through SRS and SSFS effects, the infrared edge will be limited by the silica loss, and the visible edge will also be limited through the group-velocity match. In addition, it is important to note that the generated SC in this circumstance can be noisy. This is because the SC are pumped by long pulses which is initiated by MI, both when pumped just above the ZDW [31] and just below the ZDW [32].

The time domain characteristics of the output were measured using an InGaAs photodetector (5 GHz bandwidth) and a broadband oscilloscope (Tektronix, MSO54). A series of regular pulses with pulse width of tens of nanoseconds can be observed in Figs. 7 and 8. And the pulse repetition rate increased almost linearly from 7 KHz to about 68 KHz by increasing the pump diode power from 1.5 W to 22.9 W. It has been confirmed that this passively Q-switched operation is mainly due to the SBS effect [33]–[35]. Through the strong optical feedback induced by the SBS, the Q factor in the cavity can be increased to several orders which result in the pulse compression and a greatly increased peak power [36]. It can be also found that the giant pulse train was not very stable which shows some intensity fluctuation and pulse interval jitter. The randomness of SBS generation might be the reason for such phenomenon, in which the threshold of the pulse generation tends to be easily influenced by the testing temperature and the strain distribution of the fiber [28]. The pulse shapes under different pump power are illustrated in Fig. 8. It seems the pulse shape don't have a relationship with the pump power, and a secondary pulse is usually accompanied with the main pulse. The secondary echo pulse is delayed by about 20∼30 ns from the main self-Q-switched pulse. Such a phenomenon is typically emerged in dynamic SBS and the delayed time is in accordance with the hypersound lifetime in silica optical fibers [37]. In this simple SC laser source, the using of PCF and the generation of high peak power nanosecond pulses are the crucial reasons for the broadband SC generation.

B. Effect of the PCF Length on SC Generation

Three different lengths (4 m, 9 m and 14 m) of PCFs are utilized here to study the effect of the fiber length on SC generation. Fig. 9 shows the spectral evolution of SC under different pump power in different fiber lengths. In this circumstances, the spectral evolution of SC is nearly the same except the output spectral bandwidth and flatness. This also demonstrate that their nonlinear evolutionary mechanisms are similar with each other. When using the 9 m and 14 m PCF, the output SC both exhibit a flat and broadband spectrum which extended a bandwidth of more than 1900 nm (from 500 nm to over 2400 nm) at the highest pump power.

Fig. 9(d) shows the relationship between the average SC output power and the input pump power. The SC output power increase linearly as the pump power increase, with the slope efficiencies of 40%, 35% and 31% for the 4 m, 9 m and 14 m long PCFs respectively. The reasons for the different conversion efficiencies are the unequal quantum defects during the spectrum and energy transfer and the different inherent absorption loss in the three sections of the PCF. Although a maximum output power of 9.2 W is obtained in the 4 m PCF, its output spectral characteristics are worse than the 9 m and 14 m counterpart. This demonstrates that the fiber length is insufficient to accumulate enough nonlinear effects for broad SC generation. In contrast, a longer fiber length can result in a broader and flatter SC output with the same pump conditions. With the increase of the fiber length, the intensity in the long wavelength region can be effectively enhanced by the soliton related effects like SSFS. Then, more dispersive waves will be captured and lead to the enhancement of the intensity in the short wavelength

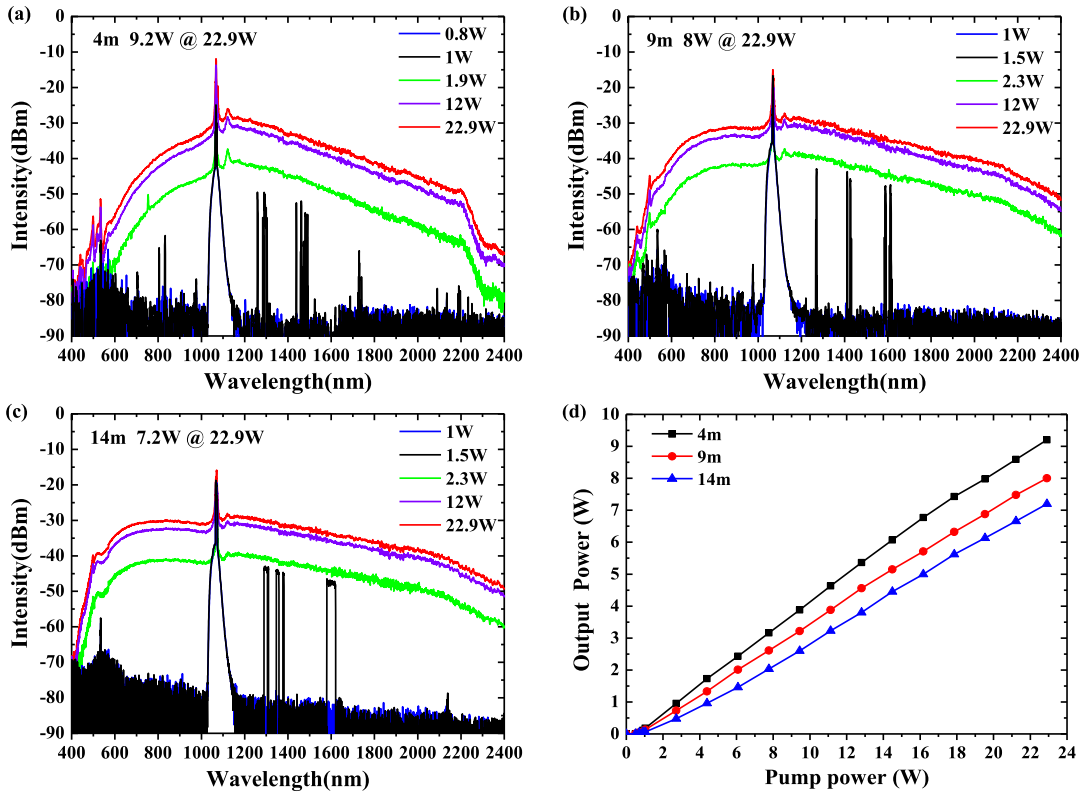

Fig. 9. The output spectra generated in different lengths of PCF: (a) 4 m, (b) 9 m, (c) 14 m. (d) Output power of SC versus the LD pump power.

side simultaneously, as shown in Fig. 9(a)-9(c). However, the increase of the fiber length will result in a lower output power and conversion efficiency. In this case, the 9 m long PCF is considered as the best choice for SC generation among the three which have a good balance between the output power and spectral broadening.

IV. Conclusion

In this paper, a high power SC with good spectral width and flatness is demonstrated in a self-Q-switched fiber laser by cascaded PCF. A flat SC with an average output power of 50.7 W and spectral range from 500 nm to beyond 2400 nm was realized, and the corresponding 20 dB bandwidth is 1900 nm except the 1064 nm peak. To the best of our knowledge, this is the highest power of SC generated in a single-stage fiber laser with such a broadband spectrum. The comparative experimental results show that an appropriate fiber length can find a good balance between the conversion efficiency and output spectra, in which the appropriate fiber length in this paper is 9 m. Compared with other SC generation methods, the method applying in this paper not only has the potential to achieve a high power SC with good spectral width and flatness, but also has the advantages of simple structure, low-cost and good robustness which may provide an easily accessible method for practical applications.

Acknowledgment

The authors would like to thank Weide Hong and Sen Guo for their valuable help in experiments.

References

[1] R. R. Alfano and S. L. Shapiro, "Emission in the region 4000 to 7000 Å via four photon coupling in glass," *Phys. Rev. Lett.*, vol. 24, pp. 584–587, 1970.

[2] J. M. Dudley and J. R. Taylor. Eds., *Supercontinuum Generation in Optical Fibers*. Cambridge, U.K.: Cambridge Univ. Press, 2010.

[3] J. M. Langridge, T. Laurila, R. S. Watt, R. L. Jones, C. F. Kaminski, and J. Hult, "Cavity enhanced absorption spectroscopy of multiple trace gas species using a supercontinuum radiation source," *Opt. Exp.*, vol. 16, no. 14, pp. 10178–10188, 2008.

[4] T. Morioka *et al.*, "1 Tbit/s (100 Gb/s 10 channel) OTDM/WDM transmission using a single supercontinuum WDM source," *Electron. Lett.*, vol. 32, pp. 906–907, May 1996.

[5] N. Nishizawa, H. Kawagoe, M. Yamanaka, M. Matsushima, K. Mori, and T. Kawabe, "Wavelength dependence of ultrahigh-resolution optical coherence tomography using supercontinuum for biomedical imaging," *IEEE J. Sel. Topics Quantum Electron.*, vol. 25, no. 1, Jul. 2019, Art no. 7101115.

[6] C. R. Petersen, P. M. Moselund, L. Huot, L. Hooper, and O. Bang, "Towards a table-top synchrotron based on supercontinuum generation," *Infrared Phys. Techn.*, vol. 91, pp. 182–186, 2018.

[7] J. C. Knight, T. A. Birks, P. St. J. Russell, and D. M. Atkin, "All-silica single-mode optical fiber with photonic crystal cladding," *Opt. Lett.*, vol. 21, pp. 1547–1549, 1996.

[8] H. Chen, S. Chen, J. Wang, Z. Chen, and J. Hou, "35 W high power all fiber supercontinuum generation in PCF with picoseconds MOPA laser," *Opt. Commun.*, vol. 284, no. 23, pp. 5484–5487, 2011.

[9] X. Qi *et al.*, "High-power visible-enhanced all-fiber supercontinuum generation in a seven-core photonic crystal fiber pumped at 1016 nm," *Opt. Lett.*, vol. 43, no. 5, pp. 1019–1022, 2018.

[10] K. K. Chen *et al.*, "Picosecond fiber MOPA pumped supercontinuum source with 39 W output power," *Opt. Exp.*, vol. 18, no. 6, pp. 5426–5432, 2010.

[11] M. Maria *et al.*, "Q-switch-pumped supercontinuum for ultra-high resolution optical coherence tomography," *Opt. Lett.*, vol. 42, no. 22, pp. 4744–4747, 2017.

[12] J. Cascante-Vindas, A. Díez, J. L. Cruz, and M. V. Andrés, "Supercontinuum Q-switched Yb fiber laser using an intracavity microstructured fiber," *Opt. Lett.*, vol. 34, no. 23, pp. 3628–3630, 2009.

[13] C. Kneis *et al.*, "High-peak-power single-oscillator actively Q-switched mode-locked Tm^{3+}-doped fiber laser and its application for high-average output power mid-IR supercontinuum generation in a ZBLAN fiber," *Opt. Lett.*, vol. 41, no. 11, pp. 2545–2548, 2016.

[14] W. Yang, B. Zhang, K. Yin, X. Zhou, and J. Hou, "High power all fiber mid-IR supercontinuum generation in a ZBLAN fiber pumped by a 2 μm MOPA system," *Opt. Exp.*, vol. 21, no. 17, pp. 19732–19742, 2013.

[15] X. Xiao and Y. Hua, "Supercontinuum generation based on all-normal-dispersion Yb-doped fiber laser mode-locked by nonlinear polarization rotation: Influence of seed's output port," *Opt. Commun.*, vol. 377, pp. 94–99, 2016.

[16] X. Qi, S. Chen, H. Sun, B. Yang, and J. Hou, "1016nm all fiber picosecond MOPA laser with 50W output," *Opt. Exp.*, vol. 24, no. 15, pp. 16874–16883, 2016.

[17] J. Travers, A. Rulkov, B. Cumberland, S. Popov, and J. Taylor, "Visible supercontinuum generation in photonic crystal fibers with a 400W continuous wave fiber laser," *Opt. Exp.*, vol. 16, no. 19, pp. 14435–14447, 2008.

[18] B. Cumberland, J. Travers, S. Popov, and J. Taylor, "Toward visible cw-pumped supercontinua," *Opt. Lett.*, vol. 33, no. 18, pp. 2122–2124, 2008.

[19] A. Kudlinski *et al.*, "White-light cw-pumped supercontinuum generation in highly GeO_2-doped-core photonic crystal fibers," *Opt. Lett.*, vol. 34, no. 23, pp. 3631–3633, 2009.

[20] A. Kudlinski, G. Bouwmans, M. Douay, M. Taki, and A. Mussot, "Dispersion-engineered photonic crystal fibers for CW-pumped supercontinuum sources," *J. Lightw. Technol.*, vol. 27, no. 21, pp. 1556–1564, 2009.

[21] B. Barviau, O. Vanvincq, A. Mussot, Y. Quiquempois, G. Mélin, and A. Kudlinski, "Enhanced soliton self-frequency shift and cw supercontinuum generation in GeO_2-doped core photonic crystal fibers," *J. Opt. Soc. Amer. B*, vol. 28, no. 5, pp. 1152–1160, 2011.

[22] C. Larsen, D. Noordegraaf, P. M. W. Skovgaard, K. P. Hansen, K. E. Mattsson, and O. Bang, "Gain-switched CW fiber laser for improved supercontinuum generation in a PCF," *Opt. Exp.*, vol. 19, no. 16, pp. 14883–14891, Aug. 2011.

[23] C. Larsen, S. T. Sørensen, D. Noordegraaf, K. P. Hansen, K. E. Mattsson, and O. Bang, "Zero-dispersion wavelength independent quasi-CW pumped supercontinuum generation," *Opt. Commun.*, vol. 290, pp. 170–174, 2013.

[24] J. He, R. Song, W. Yang, and J. Hou, "High-efficiency ultra-compact near-infrared supercontinuum generated in an ultrashort cavity configuration," *Opt. Exp.*, vol. 29, no. 12, pp. 19140–19146, 2021.

[25] A. Jin, J. Hou, S. Chen, X. Zhou, and Z. Jiang, "Broadband supercontinuum generation based on ytterbium-doped fiber amplifier seeded by self-pulsed amplified spontaneous emission source," *J. Lightw. Technol.*, vol. 33, no. 9, pp. 1850–1856, 2015.

[26] I. A. Lobach, S. I. Kablukov, E. V. Podivilov, and S. A. Babin, "Broad-range self-sweeping of a narrow-line self-pulsing Yb-doped fiber laser," *Opt. Exp.*, vol. 19, no. 18, pp. 17632–17640, 2011.

[27] P. Peterka *et al.*, "Reflectivity of transient Bragg reflection gratings in fiber laser with laser-wavelength self-sweeping," *Opt. Exp.*, vol. 22, no. 24, pp. 30024–30031, 2014.

[28] G. P. Agrawal, *Nonlinear Fiber Optics*, 5th ed. New York, NY, USA: Academic, 2013.

[29] C. Xiong, Z. Chen, and W. J. Wadsworth, "Dual-wavelength-pumped supercontinuum generation in an all-fiber device," *J. Lightw. Technol.*, vol. 27, no. 11, pp. 1638–1643, 2009.

[30] W. Gao *et al.*, "Experimental investigation on supercontinuum generation by single, dual, and triple wavelength pumping in a silica photonic crystal fiber," *Appl. Opt.*, vol. 55, no. 33, pp. 9514–9520, 2016.

[31] U. Møller *et al.*, "Power dependence of supercontinuum noise in uniform and tapered PCFs," *Opt. Exp.*, vol. 20, no. 3, pp. 2851–2857, Jan. 2012.

[32] U. Møller and O. Bang, "Intensity noise in normal-pumped picosecond supercontinuum generation, where higher-order Raman lines cross into anomalous dispersion regime," *Electron. Lett.*, vol. 49, no. 1, pp. 63–64, 2013.

[33] S. V. Chernikov, Y. Zhu, J. R. Taylor, and V. P. Gapontsev, "Supercontinuum self-Q-switched ytterbium fiber laser," *Opt. Lett.*, vol. 22, no. 5, pp. 298–300, 1997.

[34] M. Salhi *et al.*, "Evidence of Brillouin scattering in an ytterbium-doped double-clad fiber laser," *Opt. Lett.*, vol. 27, no. 15, pp. 1294–1296, 2002.

[35] A. A. Fotiadi and P. Mégret, "Self-Q-switched Er-Brillouin fiber source with extra-cavity generation of a Raman supercontinuum in a dispersion-shifted fiber," *Opt. Lett.*, vol. 31, no. 11, pp. 1621–1623, 2006.

[36] L. Pan, I. Utkin, R. J. Lan, Y. Godwal, and R. Fedosejevs, "High-peak-power subnanosecond passively Q-switched ytterbium-doped fiber laser," *Opt. Lett.*, vol. 35, no. 7, pp. 895–897, 2010.

[37] J. Bar-Joseph, A. A. Friesem, E. Lichtman, and R. G. Warris, "Steady and relaxation oscillations of stimulated Brillouin scattering in single-mode optical fibers," *J. Opt. Soc. Amer. B*, vol. 2, no. 10, pp. 1606–1611, 1985.